

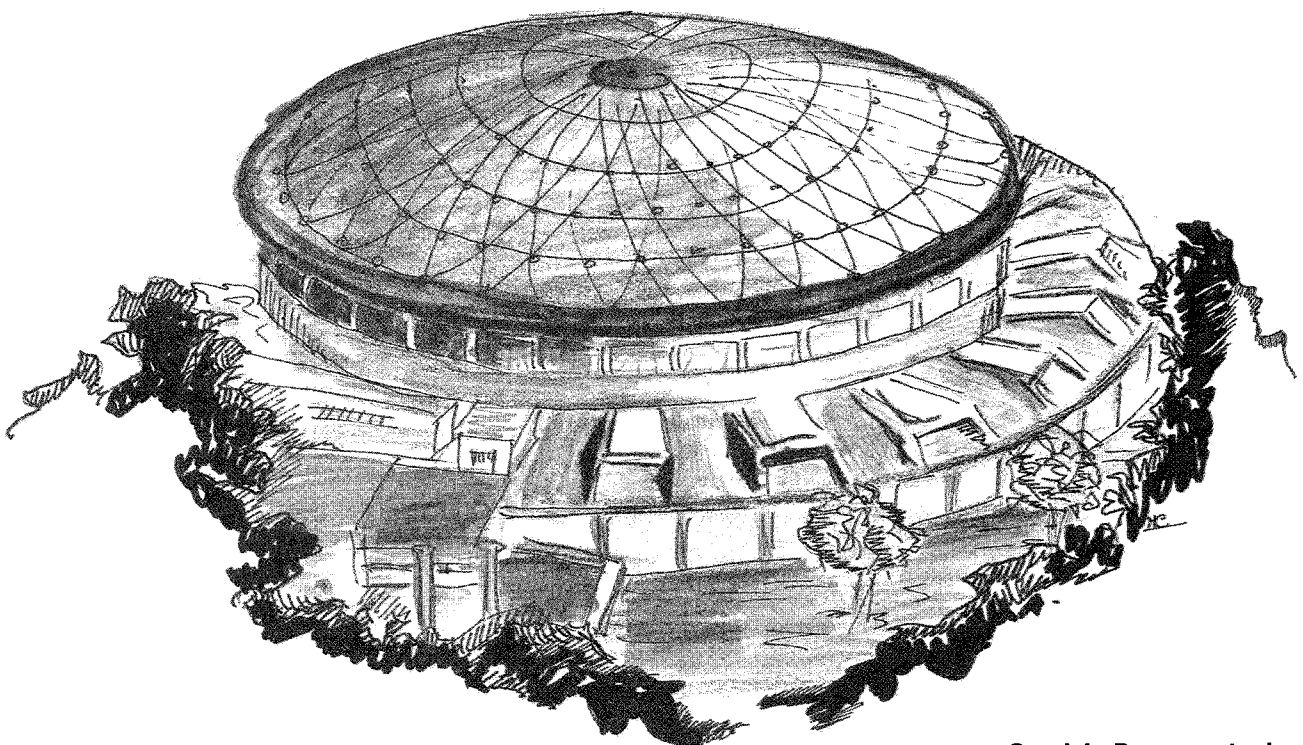


Laboratori Nazionali di Frascati

LNF-90/069(NT)
12 Settembre 1990

R. Ceccarelli, M. De Giorgi, D. Di Gioacchino, U. Gambardella, C. Vaccarezza:

CRYOGENIC REFRIGERATION OF THE LIS-A SUPERCONDUCTING CAVITIES



Servizio Documentazione
dei Laboratori Nazionali di Frascati
P.O. Box, 13 - 00044 Frascati (Italy)

CRYOGENIC REFRIGERATION OF THE LIS-A SUPERCONDUCTING CAVITIES

R. Ceccarelli, M. De Giorgi, D. Di Gioacchino, U. Gambardella, C. Vaccarezza
INFN-Laboratori Nazionali di Frascati, c.p. 13, I-00044 Frascati (Rome), Italy

ABSTRACT

The superconducting accelerating structure of the LIS-A project requires removal of about 200 W at liquid Helium temperature. To provide the requirement of a reasonable safety factor a 300 W at 4.5 K refrigerator has been foreseen. Furthermore to allow the test of high field cavities the refrigerator is upgradeable to 400 W at 4.5 K by adding a liquid Nitrogen pre-cooling. In this paper we summarize the thermodynamics aspects of the cryogenic refrigeration and the problems involved in the design of the actual refrigeration system. Some special features needed to save energy and reduce operating costs are described. The refrigeration scheme that features a distribution box between the cold box and the cryostats is described, and the flexibility features are discussed. The expected cooldown rate of a heat load under several conditions is also studied.

1- INTRODUCTION

In the framework of the realization of the LIS-A linear superconducting accelerator [1] we have studied the problem of the cryogenic refrigeration of the superconducting cavities operating at 500 MHz in a LHe bath. The refrigeration problems for RF superconducting cavities are different from those for superconducting magnets where the main contribution to the low temperature heat loads is due to thermal conductivity. In a cavity cryostat, like the one of LIS-A, the main heat load is due to the RF induced dissipations, which are about one order of magnitude larger than the static dissipations, and has to be dynamically managed.

The superconducting structure of LIS-A consists of four 4-cell cavities, each one equipped with its own cryostat. The layout of the system is shown in Fig. 1, Fig. 2 shows a schematic view of the cryostat. The mass to be cooled down for each cryostat is:

- helium dewar
st.sl. LHe tank 300 kg
Nb cavity 85 kg
Al filling bodies 450 kg
- shield
SFCu 80 K shield 110 kg

These heat loads are important for the cooldown rate of the cryostat and do not affect the steady state operation. In fact once the cavities have been cooled to the operating temperature the usual cryogenic losses due to the heat conduction, radiation, plus RF dissipations have to be considered. The RF field will induce shielding currents on the inner cavity walls. These currents, because of the presence of a surface resistance R_s , will dissipate energy on the cold walls. The liquid helium bath will adsorb this heat on the outer wall through the "thermal resistance" Z_{wall} due to the wall thickness, which is material dependent.

In our case the operating temperature T is lower than $T_c/2$, T_c being the critical temperature of Nb, and the operating frequency f is much smaller than the superconducting gap frequency ($f_{gap} \approx 700$ GHz for Niobium); the surface resistance therefore follows the usual relation [2]:

$$R_{BCS} = A(\lambda_L, \xi, l, v_F) (\omega^2/T) \exp -\{\Delta(T) / K_B T\}$$

where A is a material dependent coefficient, λ_L is the London penetration depth, ξ is the coherence length, l the mean free path, v_F is the Fermi velocity, $\Delta(T)$ is the superconducting energy gap ($\Delta(0) \approx 1.5$ meV for Niobium), K_B is the Boltzmann constant. The R_{BCS} value is in our case ≈ 70 n Ω . Experiments show that this behavior is valid to a certain limit temperature below which a finite residual surface resistance R_{res} always remains. The surface resistance R_s can therefore be expressed as a sum of two terms [3]:

$$R_s(T) = R_{BCS} + R_{res}$$

Knowing the surface resistance one can derive both the quality factor of the cavity, Q_0 (for a given geometry $Q_0 = G / R_s$, where G is the geometrical factor of the cavity), and the dissipated power within the cavity [4]:

$$P_{RF} = [E_{acc}]^2 / (z Q_0) \quad (1)$$

where E_{acc} represents the accelerating field within the cavity, and z is the cavity characteristic impedance.

The cryogenic losses are thus estimated, by using the standard relations for heat conduction and radiation [5] and Eq.1, as :

1.	Cryostat static losses at 40 + 80 K	
	-Shield radiation (surface ≈ 6.2 m ²)	12.2 W
	-Shield conduction	1.8 W
	-Supply pipe conduction	10.0 W
	-Main coupler conduction	10.0 W
	-Beam pipe conduction	25.0 W
	Total	59.0 W

2.	Cryostat static losses at 4.2 K:	
	-He tank radiation (surface 5 m ²)	0.4 W
	-He tank conduction	0.2 W
	-Main coupler	1.5 W
	-Beam pipes conduction	3.0 W

	Total	5.1 W
3.	RF dynamic losses at 4.2 K	
	- at E _{acc} = 5 MV/m and Q ₀ =2x10 ⁹	40.0 W

	Total	45.1 W

The LIS-A machine consists of four independent cavities, each in a separate cryostat. The whole structure will therefore dissipate 180.4 W in LHe, when a cooling power of 236 W is provided at the intermediate temperature shields. In the following sections we recall briefly the basic thermodynamics of the cryogenic refrigeration, the features of the adopted refrigeration system are then described, both from the point of view the thermodynamic cycle and from the point of view of operation. Finally the theoretically calculated performance on the foreseen heat load are presented.

2 - THERMODYNAMICS

The first law of thermodynamics establishes the equivalence between mechanical work and heat: the net work in a thermodynamic cycle is equal to the net heat transfer because, in a closed cycle, the initial and the final states are the same. One of the corollaries of the second law of thermodynamics is that no refrigeration system can have a Coefficient Of Performance (COP) which is larger than that of a Carnot refrigerator operating between the same two temperature limits, otherwise a perpetual motion machine of the second kind could be envisaged. It can be shown that the well known Carnot refrigerating cycle has an ideal COP, COP_{iC} where i stands for "ideal", given by [6]:

$$\text{COP}_{iC} = T_c / (T_h - T_c)$$

where $T_c (< T_h)$ and T_h are the low and the high temperature limits respectively. All cycle transformations are of course assumed to be ideal and therefore reversible.

Because of the loss of reversibility all practical refrigerators require more work for a given refrigeration effect than that required by a Carnot refrigerator working between the same temperatures. Fig.3 shows the efficiency in terms of % of COP_{iC} for several real refrigeration plants, as a function of the refrigerating capacity [7]: the higher the cooling capacity the closer the cooling system comes to the ideal Carnot efficiency (i.e. COP tends to COP_{iC}).

In several cases the cryogenic fluid is not condensed, and the energy is absorbed by the refrigerant at varying temperature, instead of at constant temperature as in the Carnot scheme. We can then imagine using an "ideal" refrigerator which absorbs heat at constant pressure: this is equivalent to infinitely many Carnot refrigerators arranged in "parallel", all with the same "sink" temperature T_h (normally the ambient temperature 300 K), but with a lower operating

temperature ranging between T_c and $T_0 > T_c$, with a temperature difference between each other of dT . The total absorbed energy between T_c and T_0 at constant pressure is then:

$$Q_a = m \{ H(T_0) - H(T_c) \}$$

where $H(T)$ is the enthalpy of the cooling fluid.

The total energy rejected from all Carnot machines, at the constant upper temperature T_h , is:

$$Q_r = m T_h \{ S(T_0) - S(T_c) \}$$

$S(T)$ being the entropy of the cooling fluid.

The first law of thermodynamics states that the work done is equal to the net heat transfer:

$$W_{net} = Q_{net} = Q_a + Q_r = m \{ T_h(S_0 - S_c) - (H_0 - H_c) \}$$

and

$$COP_i = -(Q_a / W_{net}) = (H_0 - H_c) / \{ T_h(S_0 - S_c) - (H_0 - H_c) \}$$

If the pressure and the temperature are far from the critical values the working medium may be assumed to be a perfect gas; in this case:

$$COP_i = \{ (T_0/T_c) - 1 \} / \{ (T_h/T_c) \ln (T_0/T_c) - (T_0/T_c) + 1 \} \quad (2)$$

In Fig. 4 a plot of eq. 2 is shown for several values of T_0/T_c . The thermodynamically ideal isobaric source gives a higher COP_i than the corresponding Carnot cycle when operating between the same T_h and T_c . Of course when T_0 attains T_c the COP_i value tends to the COP_{iC} .

For practical reasons (cryostat design exists and high pressure circuits within the cryostat are avoided) in our case an "isothermal" refrigerator is foreseen, that is a LHe bath. We therefore expect the cavity temperature to be very uniform.

To keep the cavities at 4.5 K the cooler has to replace all the evaporated liquid helium; a very schematic diagram of the Claude cycle is shown in Fig. 5, refrigeration power Q_a at low temperature is provided with a single expansion engine (piston or turbine). As previously shown the absorbed heat and the work done under ideal conditions are:

$$Q_a = m (H_1 - H_2) + m_e (H_3 - H_e)$$

$$-W_{net} = \dot{m} \{ T_2(S_1 - S_2) - (H_2 - H_1) \} / \epsilon_{com} - \dot{m}_e \epsilon_{exp} (H_3 - H_e)$$

where dots indicate time derivatives, \dot{m} and \dot{m}_e are the mass flow rates through the compressor and the expander respectively, ϵ_{com} and ϵ_{exp} are the compressor and the expander efficiency respectively. This expression clearly shows the connection between the COP and the mass flow rate into the expander. The working fluid makes external work on the expander thereby losing

energy, so that the closer the fluid is to a "perfect gas" (that is the higher temperature), the more it will only cool itself for the same expansion.

There are two basically types of expander: reciprocating and turbine. The choice between one of these types is a part of the more general technical problem concerning effectiveness, reliability, and costs. As previously noted the most used expander in similar refrigeration/liquefaction plants is the turbine; it is a slightly less effective than a reciprocating expander for the mass flow rate we will deal with, but gives a much higher reliability than a piston.

There are two methods to cool and keep a system at liquid Helium temperature under normal pressure, both are reported in Fig.6. In the first case (a) the Helium is first liquefied, stored into a dewar, and then subsequently or simultaneously transferred to the system to be cooled. In order to estimate the efficiency of such a process let us consider the liquefaction process on the T-S diagram shown in Fig.7, assuming Helium as the ideal working fluid. There are two contributions to the liquefaction work W_t per unit mass, the entropy and the enthalpy terms:

$$W_t = T_H \left(\int_{T_{bp}}^{T_H} \frac{C_p}{T} dT + \frac{\lambda}{T_{bp}} \right) - \left(\int_{T_{bp}}^{T_H} C_p dT + \lambda \right)$$

where T_H and T_{bp} respectively are the higher and the lower temperatures, C_p the gas thermal capacity, and λ the latent heat associated to the phase transformation. The computation yields 229 W to condense 1 liter of LHe (density $\rho \approx 125 \text{ g/dm}^3$) at $T_{bp} = 4.2 \text{ K}$ from $T_H = 300 \text{ K}$ in 1 hour. Since $\lambda = 21 \text{ J/g}$, it comes out that to produce 1 W of cooling at low temperature 315 W must be dissipated at the ambient temperature of 300 K, i.e. the efficiency is $\eta = 1/315$. When the real gas equations used, instead of the ideal $PV=nRT$, the computation yields a lower value for $\eta = 1/326$.

Looking now to the scheme of Fig.6b, where a closed cycle refrigeration is shown, it is easy to compute from a simple Carnot cycle that $\eta = T_{bp} / (T_H - T_{bp}) = 1/70.4$; the efficiency comes from using the enthalpy of the return gas to pre-cool the incoming high pressure stream by means of an ideal heat exchangers.

3 - LIS-A REFRIGERATOR

On the basis of the previous considerations we choose a closed cycle scheme for the LIS-A refrigerator. In addition the following remarks gave us further boundary conditions for an effective and reliable refrigerating plant:

1. it is cheaper to refrigerate at $4.4 \div 4.5 \text{ K}$ than at 4.2 K (which avoids lower than atmosphere pressure operation of the transfer lines and/or the use of cold compressors);
2. a system designed as a refrigerator is not optimized as a liquefier, because of the liquefier's unbalanced flow;
3. the most frequently used refrigeration plants in our range of cooling power ($\approx 300 \text{ W}$ at low temperature) use turbine expander devices.

The refrigerator we selected was a Sulzer TCF 50, capable of keeping the temperature of the cavities as low as 4.5 K while providing up to 400 W refrigeration power at this temperature, by means of liquid Nitrogen precooling.

The gas flow scheme into the cold box is shown in Fig. 8. One can see the typical serial arrangement of the turbine expanders that reduces the pressure drop across turbines. There are nine counterflow heat exchangers in the cold box, allowing to reach an efficiency of about 10% of COP_{iC} . This efficiency is in agreement with data reported in Fig. 5 [7]. To minimize the two-phase flow into the transfer lines a phase separator is integrated into the cold box, which, in addition, will also keep the low temperature dissipations constant by means of an internal heater. The heater is controlled by a LHe level control, so that the total heat (i.e. the one due to the cavities and cryostats plus the heater) is constant. This is important because variations of the cavity heat load may induce undesirable pressure fluctuations in the He circuit. In our system a constant flow is established, which makes for stable operation.

The liquid cold flow is forced through transfer lines connecting the cold box to the distribution box. The flow path of the distribution box is shown in Fig. 9. The box splits the main stream into four streams, one for each cryostat, and automatically controls the refrigeration needed by each cavity by adjusting the inlet flow. This takes place both for the 4.5 K lines and for the shield lines. All return lines (4.5 K and shield lines) are provided with normally open manual valves; this means that the LHe bath pressure inside the cryostats is the same.

In Fig. 10 is shown the compressor circuit. The gas flow scheme includes the necessary oil drain circuit, the oil adsorber, gas purifier, and the 30 m³ gas storage vessel at 12 atm. This vessel can recover, in the form of pure Helium, all the inventory needed to fill the four cryostats.

The thermodynamic cycle performed on the T-S diagram by the gas with no LN₂ precooling is shown in Fig. 11. The compressor delivers about 63.4 g/s of helium at 305 K and 13.2 bar. The pressure drop on the high pressure side of the Cold Box is about 0.2 bar, almost entirely due to the very first exchangers. The shield refrigeration is extracted from the flow of 41.1 g/s of Helium at 59 K; at the nominal power of 1000 W the temperature of this flow increases to 63.9 K, the enthalpy increase being ≈ 25 J/g. The two turbine expanders cool the stream down to 10 K. The stream will also cool the remaining 22.2 g/s stream required to provide 325 W of refrigeration at 4.5 K plus the cooling of the incoming gas from 10 to 5 K before the Joule Thomson expansion.

The plug power of the plant is ≈ 225 kW, which means about 0.5 Mlit/day of operating cost. Because dissipations at 4.5 K should be lower than the maximum available power for long periods, such as when the beam is not in operation and the cavity are kept cold (which is the best to avoid contaminations), some modifications are foreseen to run the refrigerator at lower input power.

Finally Fig. 12 shows the expected cooldown rate of the Cold Box and of one cryostat. It has been calculated using the data reported of section 1, neglecting RF induced dissipations, and considering the cooling capacity of the refrigerator without LN₂ precooling. It can be seen from the graph that it will take more than 20 hours to reach the operating temperature.

REFERENCES

1. A. Aragona, C. Biscari, R. Boni, M. Castellano, A. Cattoni, V. Chimenti, S. De Simone, G. Di Pirro, S. Faini, U. Gambardella, A. Ghigo, S. Guiducci, S. Kulinski, L. Maritato, G. Modestino, P. Patteri, M. A. Preger, C. Sanelli, M. Serio, B. Spataro, S. Tazzari, F. Tazzioli, L. Trasatti, M. Vescovi, N. Cavallo, F. Cevenini, "The Linear Superconducting Accelerator project LISA", Proc. 1st European Particle Accelerator Conference, Rome, June 7-11, 1988
2. D.C. Mattis, J. Bardeen, Phys. Rev. **111** (1958) 412
3. J. Halbritter, Z. Phys **238** (1970) 466
4. H. Piel, internal report CERN 89-04
5. G. K. White, "Experimental Techniques in Low-Temperature Physics", Clarendon Press, Oxford, 1979
6. R. Barron, "Cryogenic Systems", McGraw Hill Book Company, 1974
7. T.R. Storbridge, "Cryogenic refrigerators: an update survey", NBS technical note 655 (1974)

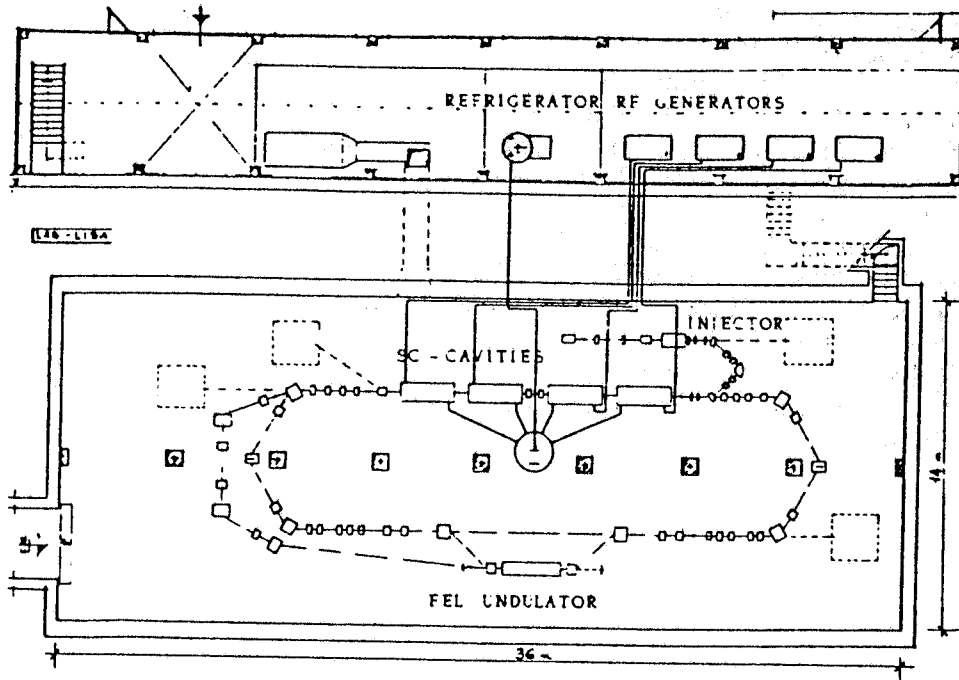


FIG. 1 - General lay-out of the LIS-A superconducting linac.

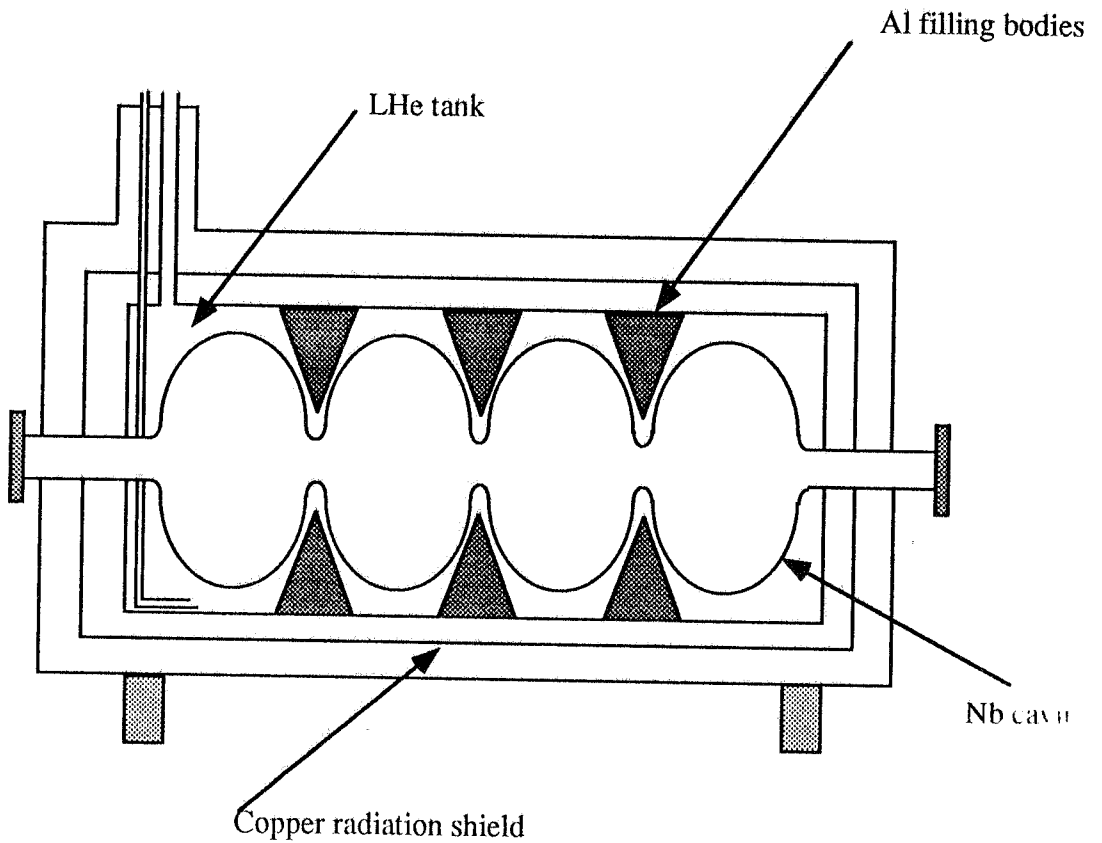


FIG. 2. -Sketch of the cryostat and cavity assembly.

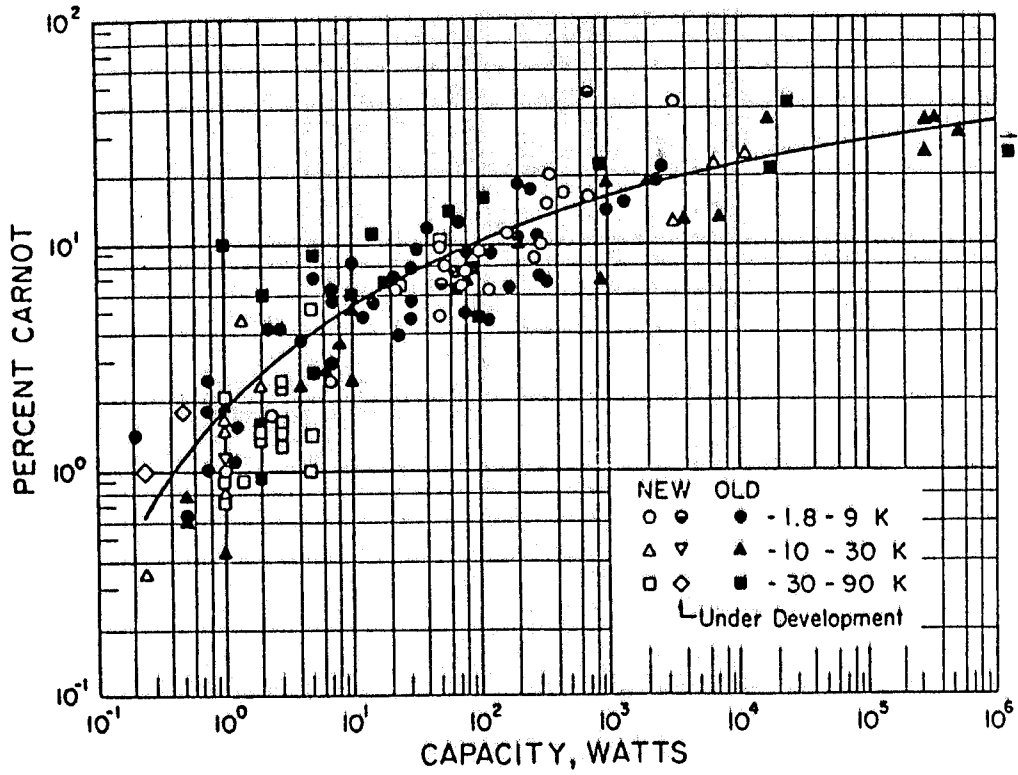
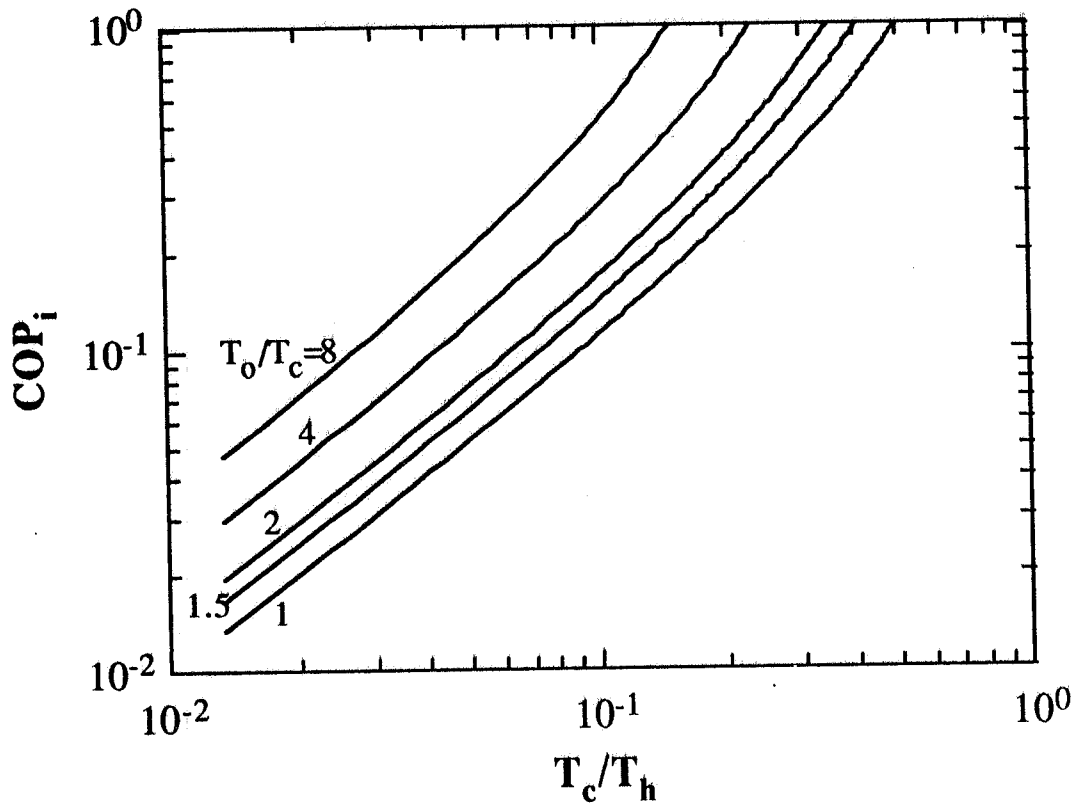


FIG. 3.- COP size effect .

FIG. 4.- COP_i for isobaric refrigeration.

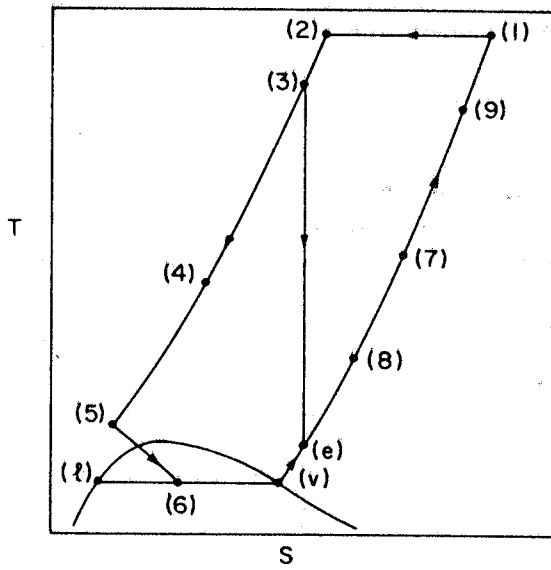
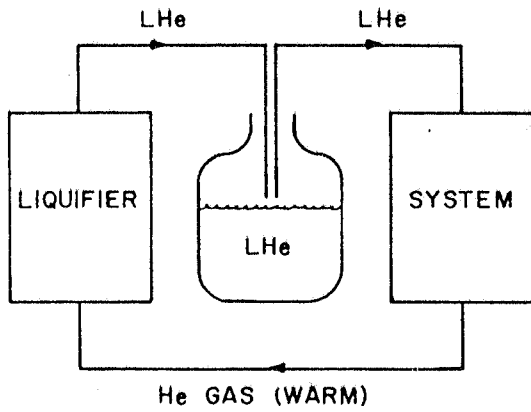
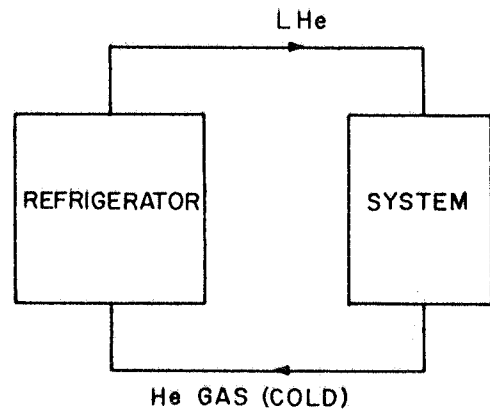


FIG. 5.- Simple Claude cycle on T-S diagram.



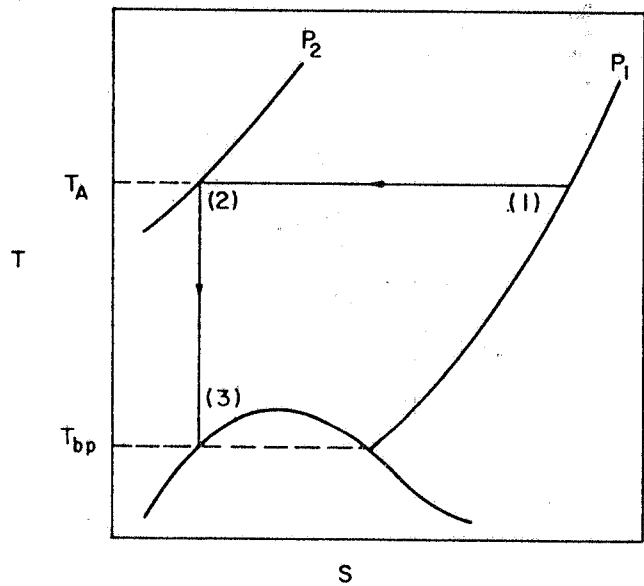
OPEN CYCLE REFRIGERATOR



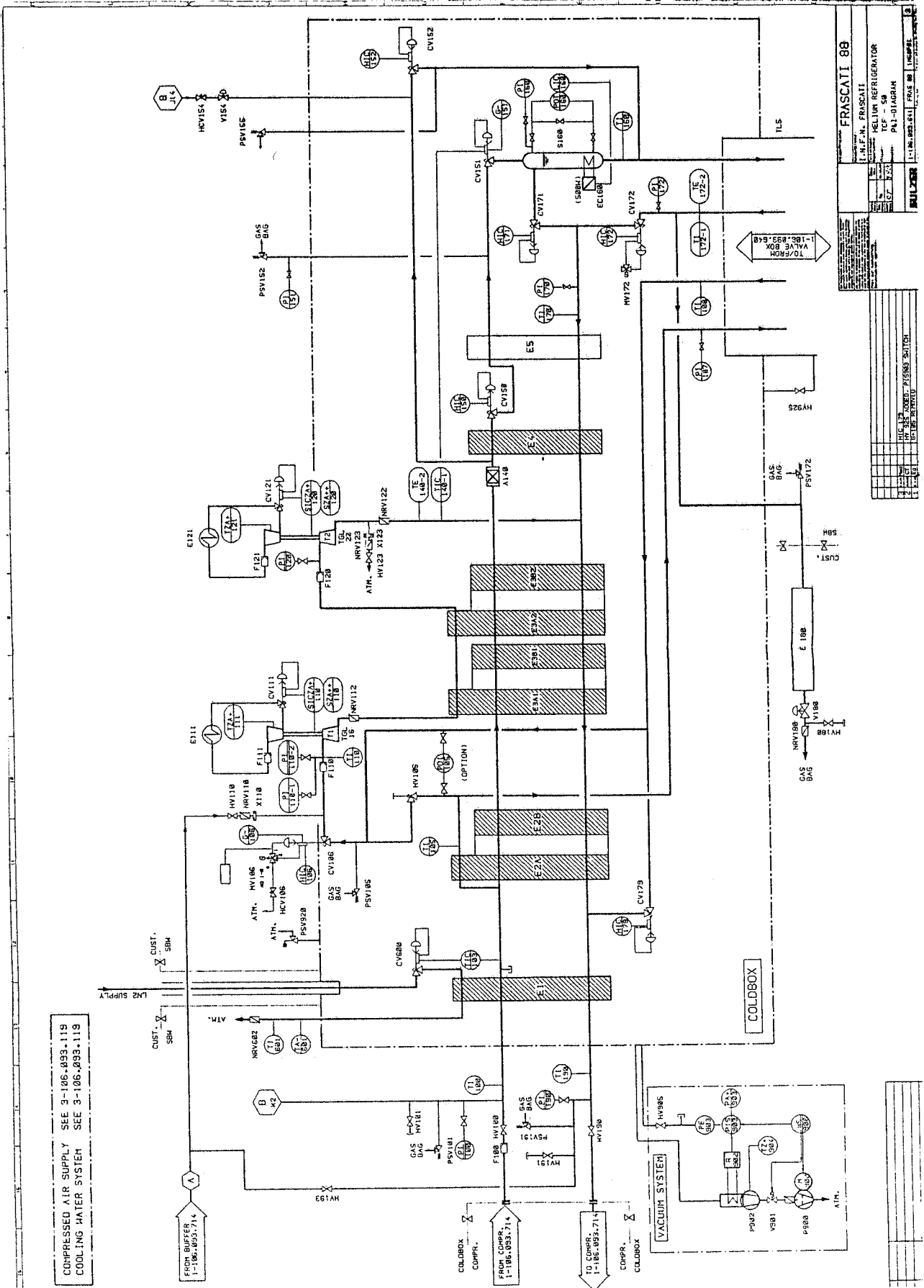
CLOSED CYCLE REFRIGERATOR

FIG. 6. - Refrigeration with open and closed cycle.

FIG. 7. - Ideal liquefaction process on T-S diagram.



S



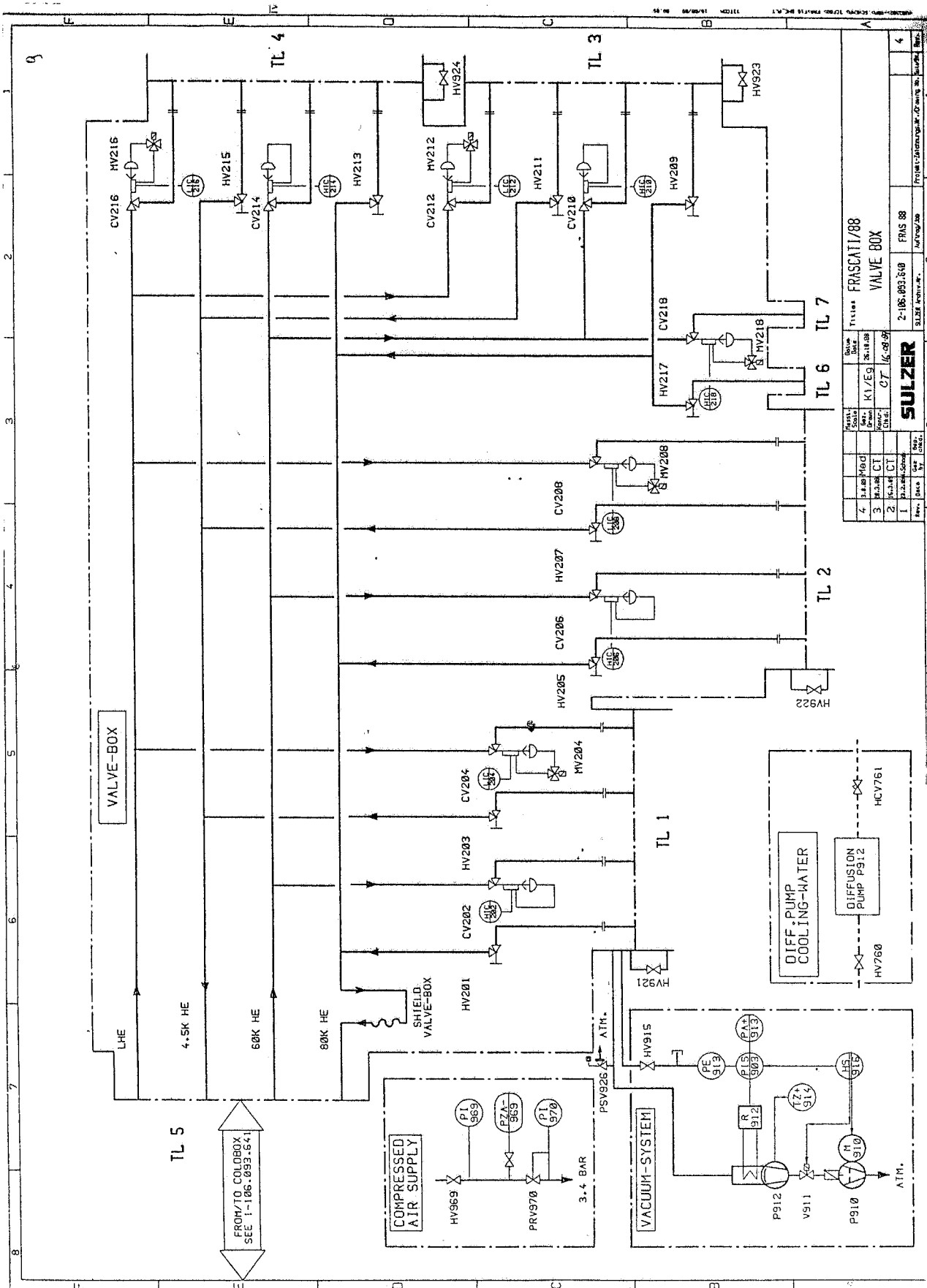


FIG. 9 - Valve Box block diagram.

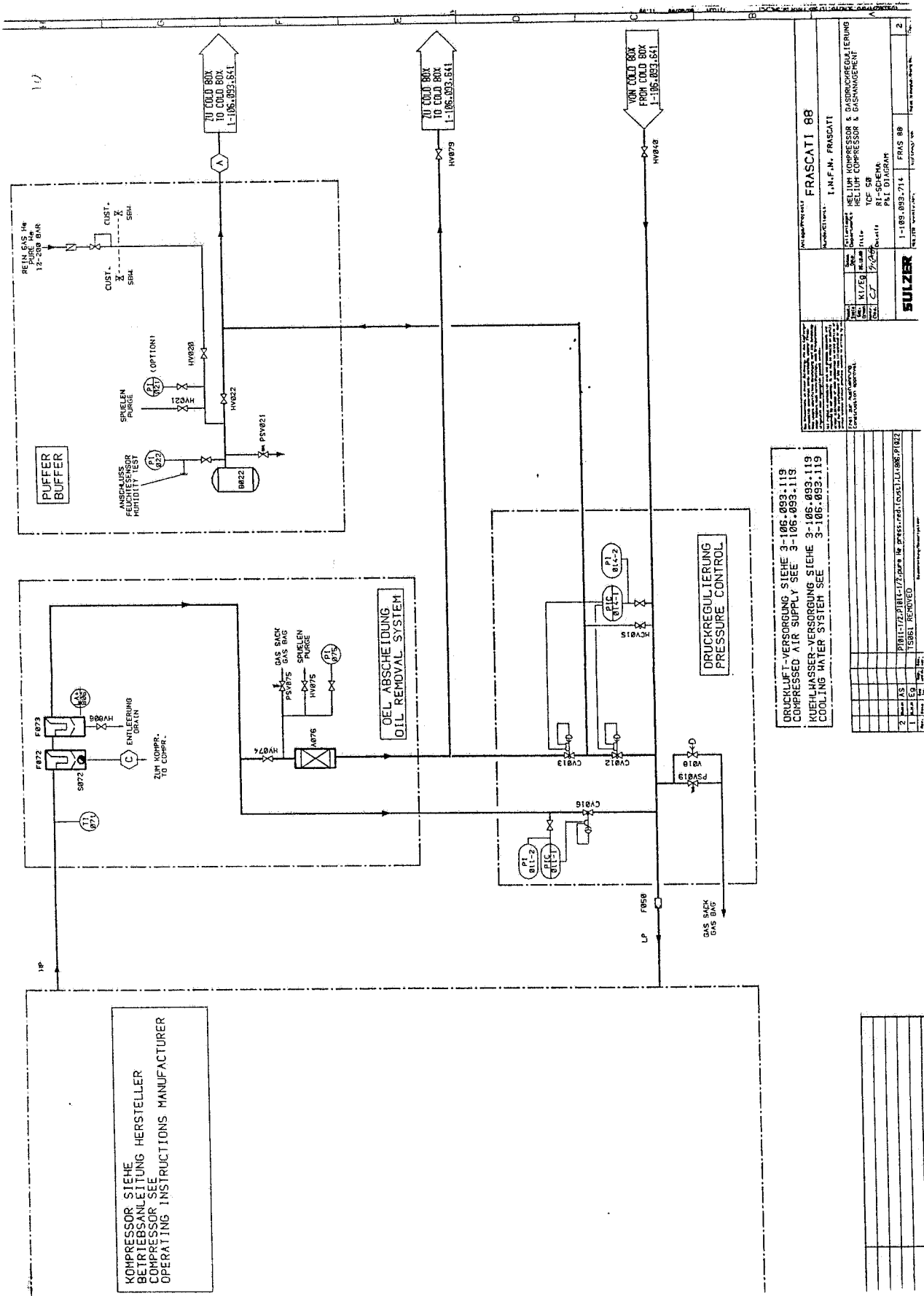


FIG. 10 - Compressor ancillary equipment.

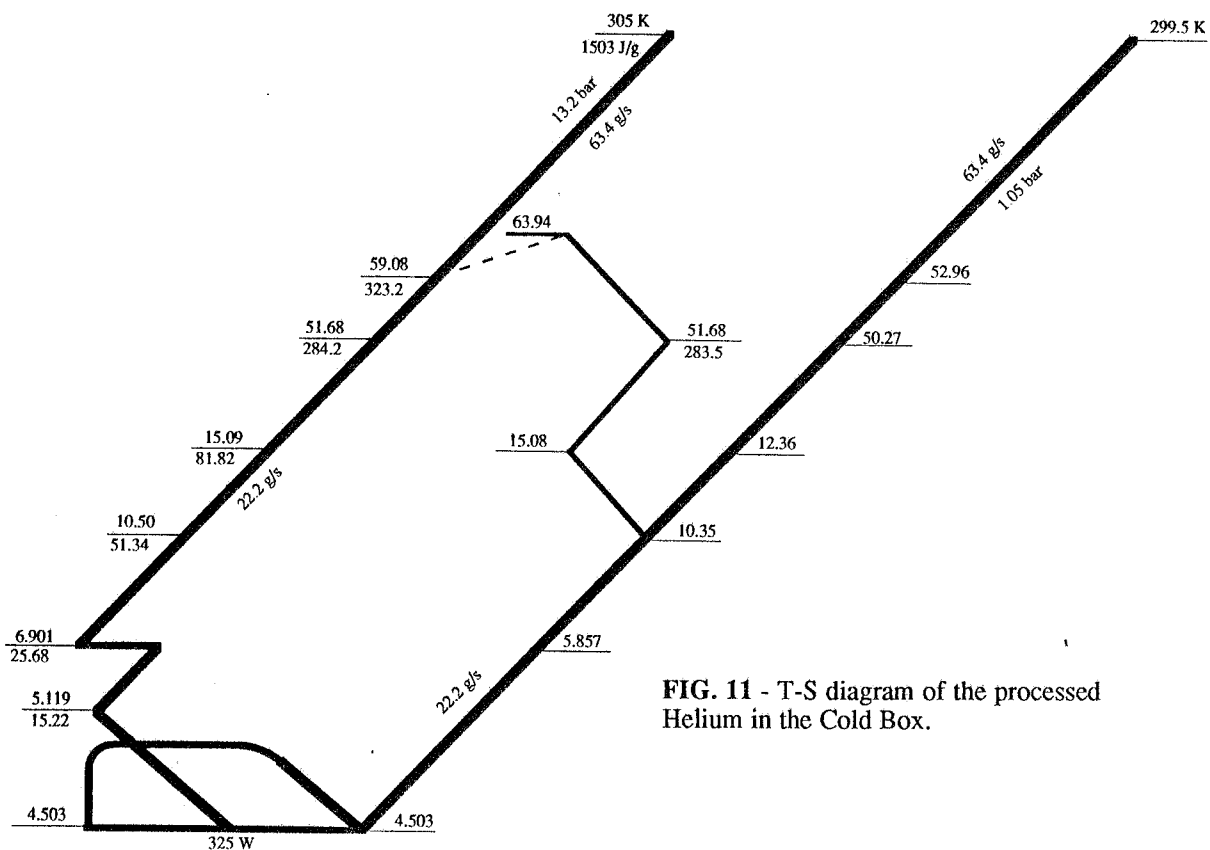


FIG. 11 - T-S diagram of the processed Helium in the Cold Box.

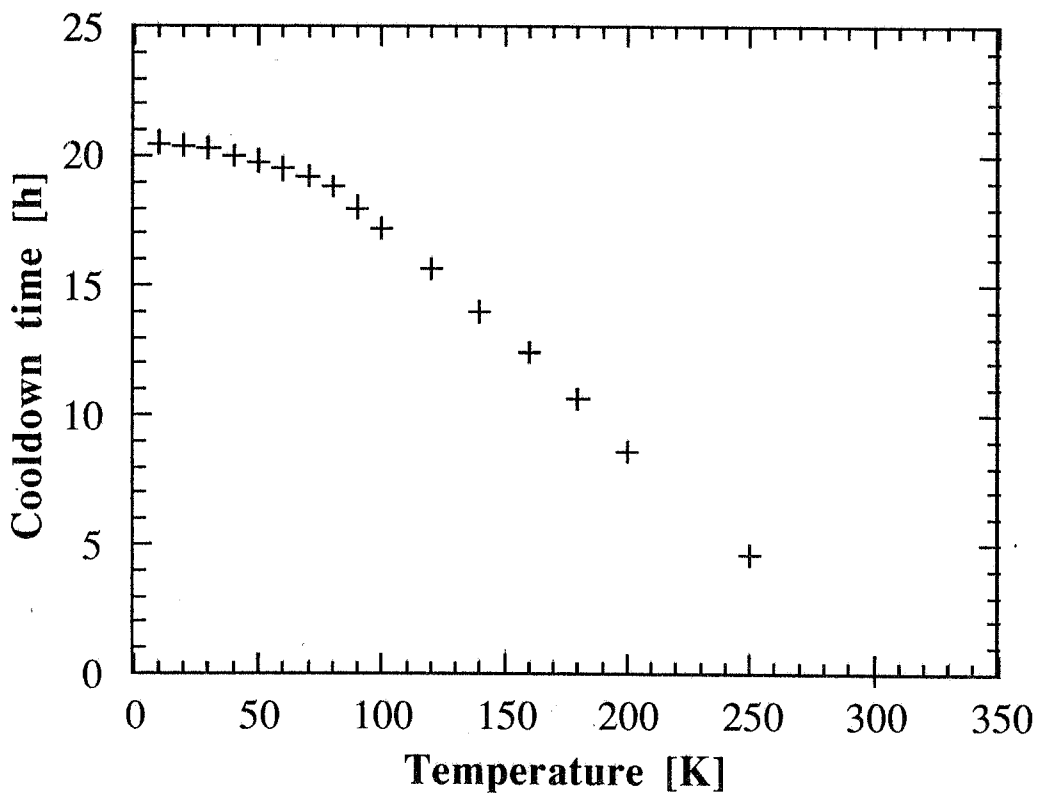


FIG. 12 - Theoretical cooldown rate of the Cold Box plus one LIS-A cryostat.